Published in final edited form as:
Mol Cancer Ther. 2013 December ; 12(12): 2827–2836. doi:10.1158/1535-7163.MCT-13-0383.

Cytoreductive Chemotherapy Improves the Biodistribution of Antibodies Directed Against Tumor Necrosis in Murine Solid Tumor Models

Julie K. Jang[1,*], **Leslie A. Khawli**[1,2,*], **Ryan Park**[1,3], **Brian W. Wu**[1], **Zibo Li**[3], **David Canter**[1], **Peter S. Conti**[3], and **Alan L. Epstein**[1]

[1]Departments of Pathology, Keck School of Medicine of University of Southern California, Los Angeles, CA

[2]Research and Early Development, Genentech, One DNA Way, South San Francisco, CA

[3]Molecular Imaging Center, Department of Radiology, University of Southern California, Los Angeles, CA

Abstract

Current strategies in cancer treatment employ combinations of different treatment modalities, which include chemotherapy, radiotherapy, immunotherapy, and surgery. Consistent with that approach, the present study demonstrates how chemotherapeutic agents can potentiate the delivery of radiolabeled, necrosis-targeting antibodies (chTNT-3, NHS76) to tumor. All chemotherapeutics in this study (5-fluorouracil, etoposide, vinblastine, paclitaxel, and doxorubicin) resulted in statistically significant increases in tumor uptake of radiolabeled antibodies and their F(ab')2 fragments compared to no pretreatment with chemotherapy. Labeled antibodies were administered at various time points following a single dose of chemotherapy in multiple tumor models, and the biodistribution of the antibodies were determined by measuring radioactivity in harvested tissues. MicroPET/CT was also done to demonstrate clinical relevancy of using chemotherapy pretreatment to increase antibody uptake. Results of biodistribution and imaging data reveal specific time frames following chemotherapy when necrosis-targeting antibodies are best delivered, either for imaging or radiotherapy. Thus, the present work offers the prospect of using cytoreductive chemotherapy to increase tumor accumulation of select therapeutic antibodies, especially when combined with other forms of immunotherapy, for the successful treatment of solid tumors.

Keywords

biodistribution; imaging; antibody uptake; cytotoxic drugs; necrosis

Introduction

Monitoring therapy in patients with solid tumors is often difficult and unreliable. The response to treatment generally is monitored using computer tomography (CT) or magnetic resonance imaging (MRI) scans, positron emission tomography (PET) scans using ^{18}F-

[1]To whom correspondence should be addressed: Alan L. Epstein, M.D., Ph.D., Department of Pathology, University of Southern California, Keck School of Medicine, 2011 Zonal Avenue, HMR 205, Los Angeles, CA 90033; Phone: (323) 442-1172; aepstein@usc.edu.

[*]These authors contributed equally to the study.

The authors disclose no potential conflicts of interest.

fluorodeoxyglucose (^{18}F-FDG) (1, 2), or by measuring tumor markers present in the serum, such as CEA in colon (3) and breast cancer (4) or PSA in prostate cancer (5). In most situations, it takes 4-6 weeks before a difference in tumor size is appreciated by CT or MRI, while in the case of serum measurement, there are only a few markers currently available (3, 4, 6). Under current methods, patients are required to complete a full course of therapy before they are monitored for tumor reduction (1-3). Because of the associated toxicity of combination chemotherapy, there is a dire need to monitor the response to therapy promptly. With that need in mind, our laboratory previously discovered that tumor necrosis can be targeted using monoclonal antibodies, designated Tumor Necrosis Therapy (TNT), directed against universally present, stable antigens retained by necrotic cells. Since necrosis is an early result of successful therapy, TNT can be used to monitor cytoreductive therapies by pre- and post-therapy imaging. As opposed to imaging with ^{18}F-FDG, where response to therapy is reflected in decreased ^{18}F-FDG uptake, increased TNT signaling is expected to increase with successful therapy and can be used more immediately following therapy.

Since discovering this approach, we continued to generate new antibodies that have improved uptake in necrotic and degenerating areas of tumors. Two chimeric TNT antibodies, chTNT-1 and chTNT-3, were developed and binding studies confirmed that chTNT-3 is principally directed against single-stranded DNA and RNA, and does not cross react with chTNT-1, which is directed against structures in the nucleosomes (7, 8). In addition, a human TNT-1 antibody, designated NHS76, has been generated using phage display methods (9). Unlike ^{18}F-FDG, which is solely used for imaging tumors by PET, radiolabeled TNT are currently in clinical trials for therapy of recurrent solid tumors including lung carcinomas and brain cancers. These ongoing clinical studies have provided strong evidence that TNT specifically target tumors in patients and are able to deliver radiation to the tumor site (10-12). Because TNT are also ideal imaging and due to their ability to target the majority of human and animal solid tumors, we developed chTNT-3 single chain derivatives (scFv, diabody and triabody), and Fab and F(ab')$_2$ fragments that clear rapidly yet retain their ability to localize to tumors (13, 14).

In addition, our laboratory has pioneered the use of antibody immunoconjugates, such as IL-2 fusion proteins, to induce transient vasopermeability in tumor vessels (15-17). This approach aims at altering the physiologic state of tumor vessels to enhance the tumor uptake of monoclonal antibodies and other macromolecules. These vasoactive reagents can be used to potentiate the effects of chemotherapy on the pharmacokinetics of drugs and antibodies administered subsequently (15-17).

In this paper, we show that TNT has better uptake following chemotherapy pretreatment. The addition of targeted-IL-2 to the chemotherapy pretreatment further improved TNT uptake. More importantly, we show that enhanced uptake following chemotherapy is optimal at different times depending on the drug being used. For these studies, TNT antibodies (chTNT-3, NHS76), and chTNT-3 F(ab')2 were characterized *in vivo* to define their pharmacokinetic properties before and after chemotherapy in solid tumor-bearing mice. chTNT-3 was also investigated with microPET/CT to illustrate how this approach can be translated to clinical imaging of tumors. It is anticipated that these biodistribution and imaging studies will form the basis of future clinical trials designed to monitor the effects of cytoreductive therapies by imaging necrotic responses and/or increase uptake of therapy-delivering antibodies in solid tumor patients.

Materials and Methods

Reagents

chTNT-3 (IgG_1), chTNT-3 F(ab')2, and human monoclonal antibody NHS76 (IgG_1) were genetically engineered, expressed, and purified as described previously (8, 9, 13, 14). The fusion protein, designated chTNT-3/IL-2, was constructed and expressed in NSO cells using the glutamine synthetase expression system (15, 18). Sulfo-NHS (*N*-hydroxysulfosuccinimide) and EDC (ethyl(dimethylaminopropyl) carbodiimide) were purchased from Sigma-Aldrich Co. (St. Louis, MO). 1,4,7,10-tetraazacyclododecane-1,4,7,10-tetraacetic acid (DOTA) was purchased from Macrocyclics, Inc. (Dallas, TX). BaBaSar is available from KeraFast (Boston, MA) (19). Size exclusion PD-10 columns were purchased from GE Healthcare. Copper-64 (^{64}Cu) was obtained from Washington University (St. Louis, MO) and University of Wisconsin (Madison, WI). All chemotherapeutic drugs including 5-fluorouracil (5-FU), paclitaxel, doxorubicin, vinblastine, and etoposide (VP-16) were purchased from Sigma-Aldrich Co. (St. Louis, MO).

In Vitro Studies

Radiolabeling Antibodies with ^{125}I—Purified chTNT-3, chTNT-3 F(ab')2, and NHS76 monoclonal antibodies were radiolabeled with iodine-125 (^{125}I) using the modified chloramines-T method (8, 13, 20). Briefly, 200 μCi of ^{125}I and 20 μl of an aqueous solution of chloramine-T (2 mg/ml) were added to 100 μg of antibody in 100 μl PBS. The solution was quenched after 2 min with 20 μl of sodium metabisulfite. Each reaction mixture was purified using a Sephadex G-25 column and yielded about 85-90% recovered radiolabeled products. The radiolabeled antibody preparations were diluted with PBS for injection, stored at 4°C, and administered within 2 h after labeling. Radioiodinated antibodies were analyzed using an analytical Instant Thin Layer Chromatography (ITLC) system consisting of silica gel impregnated glass fiber (Gelman Sciences, Ann Arbor, MI). Strips (2 × 20 cm) were activated by heating at 110 °C for 15 min prior to use, spotted with 1 μl of sample, eluted with methanol/H_2O (80:20), and analyzed for protein-bound and free radioiodine.

Radiolabeling Antibodies with ^{64}Cu—Amino groups on the lysine side chain of chTNT-3 were conjugated with DOTA to form DOTA-chTNT-3. In brief, DOTA was activated by EDC and Sulfo-NHS for 30 min at pH 5.5 with a molar ratio of DOTA:EDC:Sulfo-NHS at 10:5:4 to synthesize DOTA-OSSu as reported previously (21, 22). Without purification, DOTA-OSSu was cooled to 4 °C and added to the chTNT-3 in 0.1 M borate buffer, pH 8.5. The molar ratios of chTNT-3 to DOTA-OSSu were 1:2, 1:5, 1:10, and 1:20. The reaction mixtures were incubated at 4 °C overnight. The DOTA-chTNT-3 was then purified using PD-10 columns.

For chTNT-3 conjugated to a sarcophagine cage (Sar-chTNT-3), amino groups on the lysine side chain of chTNT-3 were conjugated with the bifunctional chelator BaBaSar. BaBaSar-*N*-hydroxysulfosuccinimidyl (BaBaSar-OSSu) was synthesized by activating BaBaSar with EDC and Sulfo-NHS at a molar ratio of 5:5:4 as reported previously (19, 23). Without purification, BaBaSar-OSSu was cooled to 4 °C and added to chTNT-3 in 0.1 M borate buffer, pH 8.5. The molar ratio of chTNT-3 to BaBaSar-OSSu was 1:5. The reaction mixture was incubated at 4 °C overnight and the BaBaSar-chTNT-3 was then purified using PD-10 columns.

All ^{64}Cu labeling reactions for DOTA-chTNT-3 and Sar-chTNT-3 were performed using the same protocol (23). In brief, 100–200 μg DOTA-chTNT-3 or BaBaSar-chTNT-3 were loaded with $^{64}CuCl_2$ (37–74 MBq ^{64}Cu per 50 μg antibody) in 0.1 N ammonium acetate

buffer, pH 5.5. The reaction mixture was incubated for 1 h at 40°C with constant shaking. The ^{64}Cu labeled antibody conjugates were then purified by PD-10 columns. The radioactive fractions containing ^{64}Cu-DOTA product was collected for subsequent *in vitro* and *in vivo* experiments.

Immunoreactivity and Stability of Radioimmunoconjugates—The *in vitro* immunoreactivities of radiolabeled chTNT-3, F(ab')2, and NHS76 preparations were evaluated by an indirect fixed cell radioimmunoassay using Raji cells (ATCC, Manassas, VA) developed in our laboratory for TNT antibodies (7). The *in vitro* serum stability of radiolabeled antibodies was also evaluated to determine whether deiodination occurs in the presence of serum. For this study, each radiolabeled antibody was incubated in triplicate in fresh mouse serum at 100 μg/ml at 37°C in a humidified incubator with 5% CO_2. At 0, 1, 3, 5, and 8 days, protein-bound radioactivity was determined by adding 900μl of 10% trichloroacetic acid to 100 μl aliquots of radiolabeled antibody in serum. After 5 min incubation at room temperature, protein precipitates were recovered by centrifugation, and the radioactivity in 500 μl of supernatant was determined using a gamma counter.

Pharmacokinetics and Biodistribution Studies

Tumor Models—The Madison 109 (MAD109) murine lung adenocarcinoma cell line was obtained from the National Cancer Institute (Frederick, MD) in 1990. The Colon 26 murine colorectal adenocarcinoma and the LS174T human colon tumor cell lines were obtained from ATCC (Manassas, VA) in 1999 and 1989, respectively, and authenticated by short tandem repeat profiling in 2013 (ATCC and Promega, Madison, WI). Cell lines were cultured in RPMI-1640 medium supplemented with 10% fetal bovine serum (Hyclone, Logan, UT), L-glutamine, penicillin G, and streptomycin. Normal BALB/c and athymic nude mice were purchased from Harlan Sprague Dawley (San Diego, CA). Institutional Animal Care and Use Committee approved protocols, and institutional guidelines for the proper humane care and use of animals in research were followed in all experiments.

To heterotransplant the LS174T human colon carcinoma cell line, a 0.2 mL inoculum containing 3×10^6 cells was subcutaneously injected in the left flank of 6-week-old female athymic nude mice. The tumors were grown for 14-18 days until they grew to approximately 1 cm in diameter. For the Colon 26 and MAD109 models, BALB/c mice were injected with a 0.2 ml inoculum containing 3×10^6 tumor cells subcutaneously in the left flank. The tumors were grown for 7-10 days until they reached approximately 1 cm in diameter.

Chemotherapeutic Drugs Pretreatment—Animal studies were performed to determine tumor uptake of the ^{125}I-labeled chTNT-3, ^{125}I-labeled F(ab')2, or ^{125}I-labeled NHS76 antibody before and after chemotherapy drugs, including 5-FU (50 mg/kg), doxorubicin (10 mg/kg), VP-16 (30 mg/kg), paclitaxel (20 mg/kg), and vinblastine (1.4 mg/kg). Dosing was modified from previous studies (17). Separate groups of tumor-bearing animals (n=4-5) were given intraperitoneal (i.p.) injections of drugs dissolved in 1 ml PBS at different times prior to a single intravenous (i.v.) dose of ^{125}I-labeled antibody (20 μCi/10 μg). In all the experiments, the animals were sacrificed at different times (1-5 days) for biodistribution analyses, where blood, lung, liver, spleen, stomach, kidney and tumor were weighed and measured for radioactivity with a 1282 Compugamma Counter (LKB Wallac; Victoria, Australia) (14, 20). For each mouse tissue or organ, the data were expressed as the percentage of injected dose/gram of tissue.

Combined Vasopermeability Enhancing Agents and Chemotherapy Pretreatment—The ability of combining chTNT-3/IL-2 and chemotherapeutic drugs to increase tumor uptake of antibodies directed against DNA, was examined in the MAD109

tumor model. In these studies, MAD109-bearing BALB/c mice were injected i.v. with chTNT-3/IL-2 2.5 h before the i.p. injection of VP-16 (30 mg/kg) or vinblastine (1.4 mg/kg), followed 1 d later with ^{125}I-labeled chTNT-3 (20 μCi/10 μg). The effect of chemotherapeutic drugs with and without chTNT-3/IL-2 pre-treatment on tumor uptake was evaluated by biodistribution analyses performed 3 days after the administration of ^{125}I-labeled chTNT-3 as described above.

Imaging Studies

Whole body imaging studies were performed at the USC Molecular Imaging Center. For these studies, 6-week-old female BALB/c mice were prepared in a similar manner as the biodistribution experiments. Three × 10^6 MAD109 cells were injected subcutaneously in the right flanks and allowed to grow to approximately 1 cm diameter. Mice received VP-16 (30 mg/kg) either 5 d, 3 d, or 2 d before i.p. delivery of ^{64}Cu-Sar-chTNT-3 (100 μCi). Phosphate buffered saline was used as a control for mice receiving no pretreatment.

Micro-Positron Emission Tomography (PET) and Computed Tomography (CT) imaging were acquired using the Genesys^4 (Sofie Biosciences, Culver City, CA) and InveonCT (Siemens Medical Solutions USA Inc., Knoxville, TN) scanners, respectively. Mice were anesthetized with 2% isoflurane in oxygen during induction of anesthesia, injections, and throughout microPET/CT scans. Animals were administered intravenously with 100 μCi of ^{64}Cu-Sar-chTNT-3. At 2 and 24 h post-administration of ^{64}Cu-Sar-chTNT-3, mice were anesthetized and placed into imaging chambers equipped with a heated coil to maintain body temperature and gas anesthesia. Scans on the Genesys^4 consisted of 20 minute acquisitions and were reconstructed with the maximum likelihood and expectation maximization (MLEM) algorithm using the Sofie Biosciences software. MicroCT data were acquired after PET scans. Scans were acquired using the Inveon Acquisition Workplace software (Siemens Medical Solutions USA Inc., Knoxville, TN) using the following settings: 80 keV, 500 uA, binx4, low magnification, 360° covered in 180 steps with two bed positions to produce a cube of 768 transaxial pixels × 923 axial pixels and a 104 μm voxel size. CT scans were reconstructed using Cobra 6.9.4 (Exxim Computing Corporation, Pleasanton, CA) into CT datasets and co-registered with the Genesys^4 microPET data using AMIDE software (http://amide.sourceforge.net/). Regions of interest were drawn over tumor and muscle from the right forelimb on decay corrected whole body coronal sections. Becquerel per volume of tissue was determined for regions of interest using AMIDE. Data are represented as tumor to muscle ratios.

H&E Staining for Necrosis

MAD109 tumors were excised from mice following imaging by PET/CT. Tumors were fixed in 10% formalin, and bisected prior to embedding in paraffin. Five micron tissue sections were stained with hematoxylin and eosin. Images were captured on a Leitz Orthoplan microscope (Wetzlar, Germany) using a Nikon DS-Fi2 camera (Melville, NY) and on a stereo microscope using a SPOT RTke camera (Spot Imaging Solutions, Sterling Heights, MI).

Statistical Analysis

Significance levels were determined using the one-way analysis of variance (ANOVA) followed by Tukey's post-hoc test or two-tailed Student's t-test as indicated. Statistical analysis was done using GraphPad Prism software (GraphPad, La Jolla, CA).

Results

Generation and Testing of Radioimmunoconjugates

All antibody preparations (chTNT-3, F(ab')2, and NHS76) showed a radiolabeling efficiency of 80-85% with ^{125}I. ITLC analysis of all ^{125}I-labeled TNT revealed an R_f value of 0 (TNT-bound) and a radiochemical purity of greater than 99%. In addition, the radiolabeled TNT were examined for deiodination in mouse serum over a five-day incubation period at 37°C. Approximately 95% of the activity was trichloroacetic acid precipitable for all the derivatives, indicating minimal release of free radioiodine over this time period.

A binding study was also conducted in which ^{125}I-labeled antibodies were incubated with fixed Raji cells, and the bound radioactivity was used to calculate the immunoreactivity compared to the respective native antibody. As expected, this study showed that all radioimmunoconjugates retained a minimum of 70% of the binding activity to fixed cells.

For radiolabeling with ^{64}Cu, different reaction ratios were tested for DOTA-chTNT-3 conjugation. The radiolabeling yields were 55.3%, 52.5%, 54.7% and 44.7% for DOTA/chTNT-3 reaction ratios of 2:1, 5:1, 10:1, and 20:1, respectively. The radiolabeling yield for Sar-chTNT-3 was 73.3%. Unlike DOTA-chTNT-3 conjugates, Sar-chTNT-3 retained 100% of binding ability compared to chTNT-3, and was therefore used in all subsequent experiments with ^{64}Cu-labeled chTNT-3 (^{64}Cu-Sar-chTNT-3).

Biodistribution and Imaging Studies

Chemotherapeutic Drug Pretreatment—In order to monitor the cytoreductive effects of chemotherapeutic drugs on tumor, the most promising TNT constructs described above were used to quantitate their uptake using biodistribution and imaging studies in tumor-bearing mice before and after chemotherapy. Single doses of different chemotherapeutic drugs such as 5-FU, doxorubicin, VP-16, paclitaxel, and vinblastine were used in tumor bearing mice. In order to determine the relationship between timing of pretreatment and tumor uptake, cytoreductive agents were injected i.p. at various times prior to i.v. delivery of ^{125}I-labeled antibody derivatives. Six representative examples of the studies are shown in Figures 1-3 which illustrate marked differences in tumor uptake of ^{125}I-labeled NHS76, chTNT-3, and F(ab')2 between the pretreated and control groups. For example, there was a statistically significant difference between ^{125}I-NHS76 uptake into Colon 26 tumors of non-pretreated mice, 4.16 ±0.27% ID/g (mean ± sd, n=5), compared to mice pretreated with 5-FU, 10.33 ± 1.02%ID/g (n=5), and mice pretreated with paclitaxel, 8.41 ± 0.33%ID/g (n-5), 2 days before receiving ^{125}I-NHS76 ($p < 0.001$, Figure 1). The data in Figures 2 and 3 also illustrate the specificity of tumor targeting with chTNT-3 and F(ab')2 and their increased uptake in pretreated MAD109 and LS174T tumors ($p < 0.001$ for Figures 2A, 2B, and 3A, $p < 0.05$ for Figure 3B). While the optimal times for TNT administration following chemotherapy varied, none of the experiments showed maximal antibody uptake with chemotherapy pretreatment given 1 day prior to antibody administration. This finding could be due to the fact that optimal tumor necrosis may take longer than 24 hours to occur and/or normal tissues may need some time to repair so as to not reduce TNT availability to tumor necrosis sites. The relationship between antibody uptake and chemotherapy pretreatment are consistent with multiple antibody formats, different tumor models, and different chemotherapeutics (Figure 1-3). Furthermore, there was no statistically significant increase in radioactivity in blood and host tissues in mice pretreated with chemotherapy compared to non-pretreated mice (Figures 1-3).

Imaging Studies—Imaging studies were also performed to demonstrate the potential of using TNT for clinical imaging of tumors. MicroPET/CT imaging of ^{64}Cu-Sar-chTNT-3 in

MAD109-bearing mice showed better uptake in tumor with VP-16 pretreatment compared to control animals receiving no pretreatment (Figure 4), and is consistent with biodistribution data shown in Figure 2A. There is a greater density of radiolabel in tumor relative to muscle in all groups, but the largest tumor/muscle ratios occurred in mice receiving pretreatment 2 and 3 days before administration of ^{64}Cu-Sar-chTNT-3 ($p < 0.001$ and $p < 0.01$, respectively, Figure 4A). Mice receiving pretreatment 5 days before administration of ^{64}Cu-Sar-chTNT-3 did not have statistically different tumor/muscle ratios from mice receiving no pretreatment, which further suggests that there is a critical window of time that ^{64}Cu-Sar-chTNT-3 should be administered following chemotherapy to maximize antibody uptake as expected.

To ensure that differences in antibody uptake are not due to differences in tumor sizes, tumors are shown in Figure 4B and were not statistically different in mass among treatment groups. Representative views of the microPET/CT scans are shown in coronal sections (Figure 4C) and whole body volume rendering (Figure 4D). Unlike the biodistribution data shown in Figures 1-3, there is signal in the liver shown by PET, which can be expected when using ^{64}Cu as opposed to ^{125}I as the radiolabel. In spite of liver uptake, microPET/CT scans clearly demonstrate the uptake of ^{64}Cu-Sar-chTNT-3 by tumors in all treatment groups, with greatest tumor uptake in mice receiving VP-16 2-3 days before ^{64}Cu-Sar-chTNT-3 administration. Not surprisingly, tumors pretreated with chemotherapy had larger areas of necrosis as shown by H&E staining (Figure 5). Necrosis is present in all tumor sections, but larger and more numerous necrotic areas were observed in tumors from mice treated 2-3 days prior with VP-16. While it is possible that other mechanisms may contribute, such as tumor vascular changes, the increase in necrosis (target) is likely responsible for the increased uptake of chTNT-3 by tumors pretreated with chemotherapy.

Combined Vasopermeability Enhancing agents and Chemotherapeutic Drugs Pretreatment—We have previously described the benefit of chTNT-3/IL-2 pretreatment in the delivery of therapeutic molecules, both antibodies and drugs, to solid tumors (15). In this study, the ability of chTNT-3/IL-2 to enhance labeled antibody uptake after chemotherapy, was examined in the MAD109 tumor model. MAD109-bearing BALB/c mice were injected i.v. with cold chTNT-3/IL-2 2.5 h before the i.p. injection of vinblastine (Figure 6A) or VP-16 (Figure 6B), followed 1 d later with i.v. delivery of ^{125}I-chTNT-3. Biodistribution analysis was performed 3 days after ^{125}I-chTNT-3 administration. Tumor uptake of radiolabel increased significantly with the administration of chTNT-3/IL-2 in combination with VP-16 or vinblastine compared to no pretreatment ($p < 0.001$) and pretreatment with chemotherapy alone ($p < 0.001$) (Figure 6). Uptake of radiolabel into normal organs was not statistically different between pretreatment with chemotherapy alone and pretreatment with chemotherapy and chTNT-3/IL-2. Although not shown here, previous studies show tumor uptake of ^{125}I-chTNT-3 following chTNT-3/IL-2 pretreatment alone to be similar to results with chemotherapy pretreatment (15). Since the chTNT-3/IL-2 vasoconjugate and chemotherapy agents have different mechanisms of action (increased vasopermeability and increased necrosis, respectively), these approaches have additive or synergistic effects in increasing TNT uptake into tumors when used together.

Discussion

In the past decade, antibodies have emerged as a key tool for both the treatment and monitoring of cancer. As a therapeutic agent, antibodies may provide direct cytotoxicity to cancer cells (e.g., trastuzumab, rituximab), inhibit a mechanism for survival of cancer cells (e.g., bevacizumab), or deliver other therapeutic agents to the tumor (e.g., trastuzumab emtansine, ibritumomab tiuxetan). While the use of antibodies in monitoring of cancer has been largely limited to the detection of serum biomarkers, antibodies are being further

developed for their use in monitoring cancer by PET imaging, such as the use of ^{111}In-caromab pendetide (ProstaScint) for the imaging of prostate cancer post-prostatectomy (24). However, the ability of antibodies to penetrate tumor tissue can limit their efficacy. Because antibodies are often used in combination with chemotherapy or with other treatments, the effects of these agents on the biodistribution and pharmacokinetics of other therapeutics must be considered. For example, while the combination of bevacizumab (anti-VEGF) and trastuzumab (anti-HER2) have made headway in clinical trials for advanced HER2$^+$ breast cancer (25), bevacizumab has also been shown to decrease accumulation of trastuzumab in the tumor due to normalization of tumor blood vessels (26, 27). Similarly, the use of bevacizumab reduced delivery of chemotherapy to tumors in non-small cell lung cancer patients (28). These two examples illustrate the importance of optimizing dosing regimens and studying the pharmacokinetic changes caused by treatment combinations.

Prevoius studies have demonstrated the use of radiolabeled TNT in therapy (10-12, 15, 18) and in the imaging of tumors (14, 29). We show here the versatility of using TNT following chemotherapy in different tumor models. While we have previously shown that TNT targets tumors (7-14), we specifically demonstrate that tumor uptake of TNT is aided by chemotherapy treatment. Furthermore the enhanced antibody uptake seen with chemotherapy pretreatment is not accompanied by increased uptake in normal tissues. Because higher tumor to normal tissue ratios are desirable for lowering systemic toxicity, increasing therapeutic potential, or increasing specificity in imaging, chemotherapy followed by TNT administration is ideal for radiotherapy or tumor monitoring by imaging. However, it should be emphasized that timing of the delivery of antibody after chemotherapy is critical to maximizing tumor uptake and therapy. We show that different cytoreductive drugs demonstrated different optimal times for TNT uptake. In our tumor models, 5-FU and paclitaxel show optimal uptake of TNT at 48 h post-treatment (Figure 1), whereas VP-16 shows optimal uptake at 72 h post-treatment (Figure 2A). While different drugs demonstrated different optimal pretreatment times for TNT uptake, they all fell in the range of 2-3 days before TNT administration. Different time frames are expected in human studies and with different dosing regimens, however, our results can be used to base future clinical trials involving patients undergoing antibody therapy post-chemotherapy.

Other methods of inducing necrosis, such as radiofrequency ablation (RFA), are also expected to increase TNT uptake in tumors. Anderson *et al.* demonstrated specificity of TNT localization to RFA sites in patients with hepatic metastasis of different histological origins (29). Their results with RFA and our results with chemotherapy show that TNT are not limited to a specific tumor type or to any one method of inducing necrosis. Similar in concept, other studies have demonstrated increased uptake and therapeutic efficacy of antibodies to intracellular tumor antigens when combined with methods of inducing necrosis, such as radiation or chemotherapy (30-32). While these studies appreciate the advantage of combining antibody therapy with radiation or chemotherapy, future studies should take into account that maximal uptake of antibodies targeting necrosis or intracellular antigens may only occur within a couple of days of necrosis pretreatment.

The effects of chemotherapy on TNT uptake are likely attributable to increases in necrosis (Figure 5). While changes in vasculature could contribute to improved antibody uptake, mean vessel densities, as assessed by CD31 staining, were not significantly different among VP-16 pretreated and non-pretreated tumors (data not shown). Studies on vascular changes would suggest that many agents would not improve the uptake of macromolecules, including antibodies, into tumors (33-38). Several agents, including VP-16 (33), doxorubicin (35), cyclophosphamide (36), methotrexate (36), dacarbazine (34), vinblastine (37), and 5-FU (36, 38), have been shown to reduce angiogenesis, blood vessel density and permeability. While these may contribute to normalization of tumor blood vessels, studies have shown that

normalization may actually decrease the uptake of antibodies into tumor (26, 27). However, the effect of chemotherapy on tumor vasculature may be dependent on mechanism of action and dosing, as few studies have demonstrated that some agents, like taxanes, increase vessel diameter and permeability (39, 40), which may increase antibody delivery to tumors. While the increase in necrosis is a likely explanation for enhanced TNT uptake due to the broad range of cytoreductive agents used, further studies can investigate how specific chemotherapeutics alters tumor interstitial pressure, availability of antigens, or penetration or retention of antibody in tumor tissue.

To improve uptake of antibody, we included in this study combining a vasoactive agent, chTNT-3/IL-2, to chemotherapy as part of the pretreatment regimen. We show that chTNT-3/IL-2 in conjunction with chemotherapy increased the uptake of antibodies into tumor tissue. IL-2 is known to enhance vascular permeability, as exemplified by its induction of vascular leak syndrome (41). Other studies have also demonstrated the effects of IL-2 on vascular permeability in tumor models (15, 16, 18, 42, 43). Pretreatment with free IL-2 increased tumor uptake of radiolabeled antibodies, but also increased uptake in normal lung, liver, spleen, and kidney in a mouse xenograft model (42). Due to non-specificity of vascular effects and toxicity, localization of IL-2 to the tumor microenvironment is ideal. With chTNT-3/IL-2 and chemotherapy pretreatment, we show no increase in ^{125}I-chTNT-3 uptake in IL-2-sensitive normal tissues such as, lung, liver, and kidneys. In agreement with our results using chTNT-3/IL-2, IL-2 conjugated to an anti-CEA antibody resulted in enhanced vascular permeability in CEA^{+} tumor but not host organs (43). The use of chTNT-3 as opposed to an antibody to a single antigen on specific tumors offers several benefits. Targeting tumor necrosis, which is a feature in all solid tumors, allows the chTNT-3/IL-2 conjugate to be used in different solid tumors and is not limited by the loss of antigen expression that can occur during tumor development, metastasis, or treatment.

Here, pretreatment with chemotherapy (vinblastine or VP16) and chTNT-3/IL-2 have additive or synergistic effects in the uptake of radiolabeled chTNT-3 into tumor tissue. Because we show that several chemotherapeutic drugs as single agents can enhance the uptake of TNT and antibody fragments, we expect that the tumor-specificity of chTNT-3/IL-2 can also be enhanced by standard chemotherapy. Because chemotherapy and therapeutic antibodies are often given in cycles, one can imagine the accumulating benefit with each cycle of chemotherapy and chTNT-3/IL-2. With each dose of chemotherapy, more chTNT-3/IL-2 would be expected to accumulate into tumor tissue. With the accumulation of chTNT-3/IL-2 in the tumor, greater vascular permeability, and therefore, greater entry of drugs and other therapeutics, with less side effects in normal tissue would be expected.

Another potential benefit of the chTNT-3/IL-2 conjugate not explored in this paper is the pivotal role IL-2 plays in stimulating lymphocytes and activating killer cells, such as natural killer and CD8^{+} cytotoxic T cells. For this reason, IL-2 is used in the treatment of melanoma and renal cell carcinoma (44). Targeting IL-2 to the tumor, not only enhances vascular permeability, but could also serve as a stimulatory molecule for immune cells at the tumor site. The combination of cytotoxic agents with immunotherapy is appealing, since some chemotherapeutic drugs can elicit and contribute to an immune response (45). This study did not study host immune responses, but future studies can explore the presence of activated immune cells in the tumor as a result of pretreatment with chemotherapy and chTNT-3/IL-2.

In this paper, we demonstrated that pretreatment with different chemotherapeutic drugs (5-FU, paclitaxel, VP-16, doxorubicin, and vinblastine) enhanced the uptake of radiolabeled TNT in several different murine solid tumor models. The inclusion of chTNT-3/IL-2 in the pretreatment further increased uptake of radiolabeled TNT. Our studies with chemotherapy and chTNT-3/IL-2 exemplify how immunotherapy is not only compatible with

chemotherapy, but also shows that the two can be used synergistically in the delivery of treatment to solid tumors. Finally, we have demonstrated that PET/CT imaging with radiolabeled TNT can be used to monitor the extent of necrosis early after drug administration to fulfill an important unmet clinical need.

Acknowledgments

The authors wish to acknowledge Jingzhong (James) Pang for the excellent technical assistance with the animal studies. This study was supported in part by grant 2R01 CA83001 from the National Cancer Institute, grant W81XWH-11-1-0466 from the Department of Defense, and Cancer Therapeutics Laboratories, Los Angeles, CA.

Financial Support: L.A. Khawli and A.L. Epstein were supported by grant 2R01 CA83001 from the National Cancer Institute.

J.K. Jang was supported by grant W81XWH-11-1-0466 from the Department of Defense.

References

1. Saba, N. Post-treatment surveillance of squamous carcinoma of head and neck. In: Basow, D., editor. UpToDate. Waltham, MA: 2013.
2. Mauch, P.; Friedberg, JW. Monitoring of the patient with classical Hodgkin's Lymphoma during and after treatment. In: Basow, D., editor. UpToDate. Wiltham, MA: 2013.
3. Jacobson, B.; Moy, B.; Farraye, F. Surveillance after colorectal cancer resection. In: Basow, D., editor. UpToDate. Waltham, MA: 2013.
4. Duffy MJ. Serum tumor markers in breast cancer: are they of clinical value? Clin Chem. 2006 Mar; 52(3):345–51. [PubMed: 16410341]
5. Lilja H, Ulmert D, Vickers AJ. Prostate-specific antigen and prostate cancer: prediction, detection and monitoring. Nat Rev Cancer. 2008 Apr; 8(4):268–78. [PubMed: 18337732]
6. Scott AM, Larson SM. Tumor imaging and therapy. Radiol Clin North Am. 1993 Jul; 31(4):859–79. [PubMed: 8337372]
7. Miller GK, Naeve GS, Gaffar SA, Epstein AL. Immunologic and biochemical analysis of TNT-1 and TNT-2 monoclonal antibody binding to histones. Hybridoma. 1993 Dec; 12(6):689–98. [PubMed: 8288270]
8. Hornick JL, Sharifi J, Khawli LA, Hu P, Biela BH, Mizokami MM, et al. A new chemically modified chimeric TNT-3 monoclonal antibody directed against DNA for the radioimmunotherapy of solid tumors. Cancer Biother Radiopharm. 1998 Aug; 13(4):255–68. [PubMed: 10850361]
9. Sharifi J, Khawli LA, Hu P, King S, Epstein AL. Characterization of a phage display-derived human monoclonal antibody (NHS76) counterpart to chimeric TNT-1 directed against necrotic regions of solid tumors. Hybrid Hybridomics. 2001; 20(5-6):305–12. [PubMed: 11839248]
10. Chen S, Yu L, Jiang C, Zhao Y, Sun D, Li S, et al. Pivotal study of iodine-131-labeled chimeric tumor necrosis treatment radioimmunotherapy in patients with advanced lung cancer. J Clin Oncol. 2005 Mar 1; 23(7):1538–47. [PubMed: 15735129]
11. Yu L, Ju DW, Chen W, Li T, Xu Z, Jiang C, et al. 131I-chTNT radioimmunotherapy of 43 patients with advanced lung cancer. Cancer Biother Radiopharm. 2006 Feb; 21(1):5–14. [PubMed: 16480326]
12. Hdeib A, Sloan A. Targeted radioimmunotherapy: the role of (1)(3)(1)I-chTNT-1/B mAb (Cotara) for treatment of high-grade gliomas. Future Oncol. 2012 Jun; 8(6):659–69. [PubMed: 22764763]
13. Khawli LA, Biela BH, Hu P, Epstein AL. Stable, genetically engineered F(ab')(2) fragments of chimeric TNT-3 expressed in mammalian cells. Hybrid Hybridomics. 2002 Feb; 21(1):11–8. [PubMed: 11991812]
14. Khawli LA, Biela B, Hu P, Epstein AL. Comparison of recombinant derivatives of chimeric TNT-3 antibody for the radioimaging of solid tumors. Hybrid Hybridomics. 2003 Feb; 22(1):1–9. [PubMed: 12713684]

15. Hornick JL, Khawli LA, Hu P, Sharifi J, Khanna C, Epstein AL. Pretreatment with a monoclonal antibody/interleukin-2 fusion protein directed against DNA enhances the delivery of therapeutic molecules to solid tumors. Clin Cancer Res. 1999 Jan; 5(1):51–60. [PubMed: 9918202]

16. LeBerthon B, Khawli LA, Alauddin M, Miller GK, Charak BS, Mazumder A, et al. Enhanced tumor uptake of macromolecules induced by a novel vasoactive interleukin 2 immunoconjugate. Cancer Res. 1991 May 15; 51(10):2694–8. [PubMed: 2021947]

17. Khawli LA, Hu P, Epstein AL. NHS76/PEP2, a fully human vasopermeability-enhancing agent to increase the uptake and efficacy of cancer chemotherapy. Clin Cancer Res. 2005 Apr 15; 11(8): 3084–93. [PubMed: 15837764]

18. Li J, Hu P, Khawli LA, Yun A, Epstein AL. chTNT-3/hu IL-12 fusion protein for the immunotherapy of experimental solid tumors. Hybrid Hybridomics. 2004 Feb; 23(1):1–10. [PubMed: 15000842]

19. Liu S, Li Z, Yap LP, Huang CW, Park R, Conti PS. Efficient preparation and biological evaluation of a novel multivalency bifunctional chelator for 64Cu radiopharmaceuticals. Chemistry. 2011 Sep 5; 17(37):10222–5. [PubMed: 21815227]

20. Khawli LA, Mizokami MM, Sharifi J, Hu P, Epstein AL. Pharmacokinetic characteristics and biodistribution of radioiodinated chimeric TNT-1, -2, and -3 monoclonal antibodies after chemical modification with biotin. Cancer Biother Radiopharm. 2002 Aug; 17(4):359–70. [PubMed: 12396700]

21. Li ZB, Cai W, Cao Q, Chen K, Wu Z, He L, et al. (64)Cu-labeled tetrameric and octameric RGD peptides for small-animal PET of tumor alpha(v)beta(3) integrin expression. J Nucl Med. 2007 Jul; 48(7):1162–71. [PubMed: 17574975]

22. Wu Y, Zhang X, Xiong Z, Cheng Z, Fisher DR, Liu S, et al. microPET imaging of glioma integrin {alpha}v{beta}3 expression using (64)Cu-labeled tetrameric RGD peptide. J Nucl Med. 2005 Oct; 46(10):1707–18. [PubMed: 16204722]

23. Li Z, Jin Q, Huang C, Dasa S, Chen L, Yap LP, et al. Trackable and Targeted Phage as Positron Emission Tomography (PET) Agent for Cancer Imaging. Theranostics. 2011; 1:371–80. [PubMed: 22211143]

24. Hardie AD, Rieter WJ, Bradshaw ML, Gordon LL, Young MA, Keane TE. Improved performance of SPECT-CT In-111 capromab pendetide by correlation with diffusion-weighted magnetic resonance imaging for identifying metastatic pelvic lymphadenopathy in prostate cancer. World J Urol. 2013 Apr 18.

25. Hurvitz S, Pegram M, Lin L, Chan D, Allen H, Dichmann R, et al. Final results of a phase II trial evaluating trastuzumab and bevacizumab as first line treatment of HER2-amplified advanced breast cancer. Cancer Res. 2009; 24:854s. Abstract #6094.

26. Pastuskovas CV, Mundo EE, Williams SP, Nayak TK, Ho J, Ulufatu S, et al. Effects of anti-VEGF on pharmacokinetics, biodistribution, and tumor penetration of trastuzumab in a preclinical breast cancer model. Mol Cancer Ther. 2012 Mar; 11(3):752–62. [PubMed: 22222630]

27. Arjaans M, Oude Munnink TH, Oosting SF, Terwisscha van Scheltinga AG, Gietema JA, Garbacik ET, et al. Bevacizumab-induced normalization of blood vessels in tumors hampers antibody uptake. Cancer Res. 2013 Jun 1; 73(11):3347–55. [PubMed: 23580572]

28. Van der Veldt AA, Lubberink M, Bahce I, Walraven M, de Boer MP, Greuter HN, et al. Rapid decrease in delivery of chemotherapy to tumors after anti-VEGF therapy: implications for scheduling of anti-angiogenic drugs. Cancer Cell. 2012 Jan 17; 21(1):82–91. [PubMed: 22264790]

29. Anderson PM, Wiseman GA, Lewis BD, Charboneau JW, Dunn WL, Carpenter SP, et al. A phase I safety and imaging study using radiofrequency ablation (RFA) followed by 131I-chTNT-1/B radioimmunotherapy adjuvant treatment of hepatic metastasis. Cancer Therapy. 2003; 1:297–306.

30. Desrues B, Lena H, Brichory F, Ramee MP, Toujas L, Delaval P, et al. Monoclonal antibody Po66 uptake by human lung tumours implanted in nude mice: effect of co-administration with doxorubicin. Br J Cancer. 1995 Nov; 72(5):1076–82. Research Support, Non-U.S. Gov't. [PubMed: 7577450]

31. Phaeton R, Wang XG, Einstein MH, Goldberg GL, Casadevall A, Dadachova E. The influence of proteasome inhibitor MG132, external radiation, and unlabeled antibody on the tumor uptake and biodistribution of (188)re-labeled anti-E6 C1P5 antibody in cervical cancer in mice. Cancer. 2010

Feb 15; 116(4 Suppl):1067–74. Research Support, N.I.H., Extramural Research Support, Non-U.S. Gov't. [PubMed: 20127955]

32. Noguchi T, Kato T, Wang L, Maeda Y, Ikeda H, Sato E, et al. Intracellular tumor-associated antigens represent effective targets for passive immunotherapy. Cancer Res. 2012 Apr 1; 72(7): 1672–82. Research Support, Non-U.S. Gov't. [PubMed: 22318866]
33. Panigrahy D, Kaipainen A, Butterfield CE, Chaponis DM, Laforme AM, Folkman J, et al. Inhibition of tumor angiogenesis by oral etoposide. Exp Ther Med. 2010 Sep; 1(5):739–46. [PubMed: 22993597]
34. Liu P, Zhang C, Chen J, Zhang R, Ren J, Huang Y, et al. Combinational therapy of interferon-alpha and chemotherapy normalizes tumor vasculature by regulating pericytes including the novel marker RGS5 in melanoma. J Immunother. 2011 Apr; 34(3):320–6. Research Support, Non-U.S. Gov't. [PubMed: 21389866]
35. Roy Chaudhuri T, Arnold RD, Yang J, Turowski SG, Qu Y, Spernyak JA, et al. Mechanisms of tumor vascular priming by a nanoparticulate doxorubicin formulation. Pharm Res. 2012 Dec; 29(12):3312–24. Research Support, N.I.H., Extramural Research Support, Non-U.S. Gov't. [PubMed: 22798260]
36. Bottini A, Berruti A, Bersiga A, Brizzi MP, Allevi G, Bolsi G, et al. Changes in microvessel density as assessed by CD34 antibodies after primary chemotherapy in human breast cancer. Clin Cancer Res. 2002 Jun; 8(6):1816–21. Clinical Trial Clinical Trial, Phase II Comparative Study Research Support, Non-U.S. Gov't. [PubMed: 12060622]
37. Sersa G, Krzic M, Sentjurc M, Ivanusa T, Beravs K, Cemazar M, et al. Reduced tumor oxygenation by treatment with vinblastine. Cancer Res. 2001 May 15; 61(10):4266–71. Research Support, Non-U.S. Gov't. [PubMed: 11358854]
38. Basaki Y, Chikahisa L, Aoyagi K, Miyadera K, Yonekura K, Hashimoto A, et al. gamma-Hydroxybutyric acid and 5-fluorouracil, metabolites of UFT, inhibit the angiogenesis induced by vascular endothelial growth factor. Angiogenesis. 2001; 4(3):163–73. Comparative Study. [PubMed: 11911014]
39. Griffon-Etienne G, Boucher Y, Brekken C, Suit HD, Jain RK. Taxane-induced apoptosis decompresses blood vessels and lowers interstitial fluid pressure in solid tumors: clinical implications. Cancer Res. 1999 Aug 1; 59(15):3776–82. Research Support, Non-U.S. Gov't Research Support, U.S. Gov't, P.H.S. [PubMed: 10446995]
40. Watts ME, Woodcock M, Arnold S, Chaplin DJ. Effects of novel and conventional anti-cancer agents on human endothelial permeability: influence of tumour secreted factors. Anticancer Res. 1997 Jan-Feb;17(1A):71–5. Research Support, Non-U.S. Gov't. [PubMed: 9066632]
41. Cotran RS, Pober JS, Gimbrone MA Jr, Springer TA, Wiebke EA, Gaspari AA, et al. Endothelial activation during interleukin 2 immunotherapy. A possible mechanism for the vascular leak syndrome. J Immunol. 1988 Mar 15; 140(6):1883–8. [PubMed: 3279124]
42. Nakamura K, Kubo A. Effect of interleukin-2 on the biodistribution of technetium-99m-labelled anti-CEA monoclonal antibody in mice bearing human tumour xenografts. Eur J Nucl Med. 1994 Sep; 21(9):924–9. [PubMed: 7995285]
43. Nakamura K, Kubo A. Biodistribution of iodine-125 labeled monoclonal antibody/interleukin-2 immunoconjugate in athymic mice bearing human tumor xenografts. Cancer. 1997 Dec 15; 80(12 Suppl):2650–5. [PubMed: 9406720]
44. Rosenberg SA, Yang JC, Topalian SL, Schwartzentruber DJ, Weber JS, Parkinson DR, et al. Treatment of 283 consecutive patients with metastatic melanoma or renal cell cancer using high-dose bolus interleukin 2. JAMA. 1994 Mar 23-30; 271(12):907–13. [PubMed: 8120958]
45. Baxevanis CN, Perez SA, Papamichail M. Combinatorial treatments including vaccines, chemotherapy and monoclonal antibodies for cancer therapy. Cancer Immunol Immunother. 2009 Mar; 58(3):317–24. Review. [PubMed: 18704409]

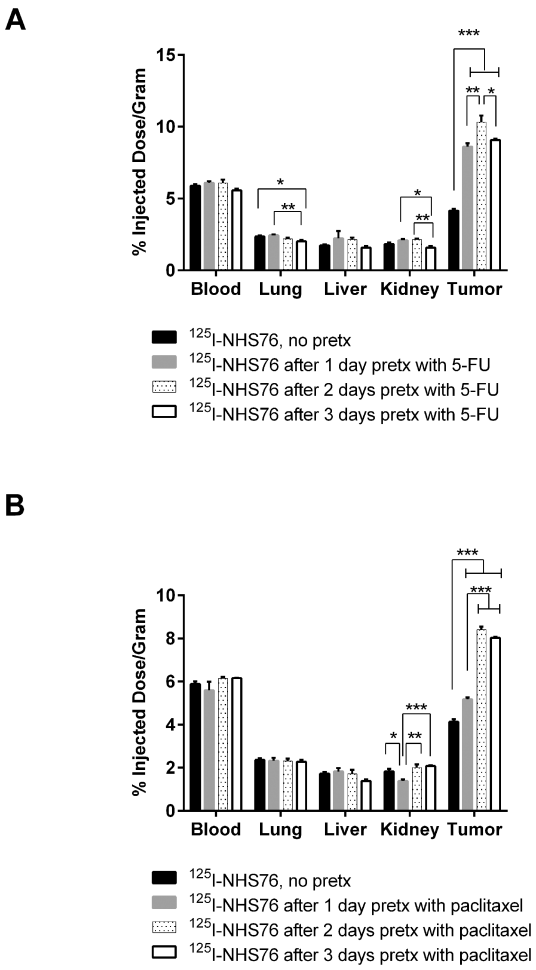

Figure 1.

Five-day biodistribution of ^{125}I-labeled NHS76 administered 1, 2, or 3 days after pretreatment with (**A**) 5-FU (50 mg/kg) and (**B**) paclitaxel (20 mg/kg) in Colon 26-bearing BALB/c mice. Error bars represent standard error of the mean. * $p < 0.05$, ** $p < 0.01$, *** $p < 0.001$ as determine using one-way ANOVA followed by Tukey's post-hoc test. N = 5 mice for all groups.

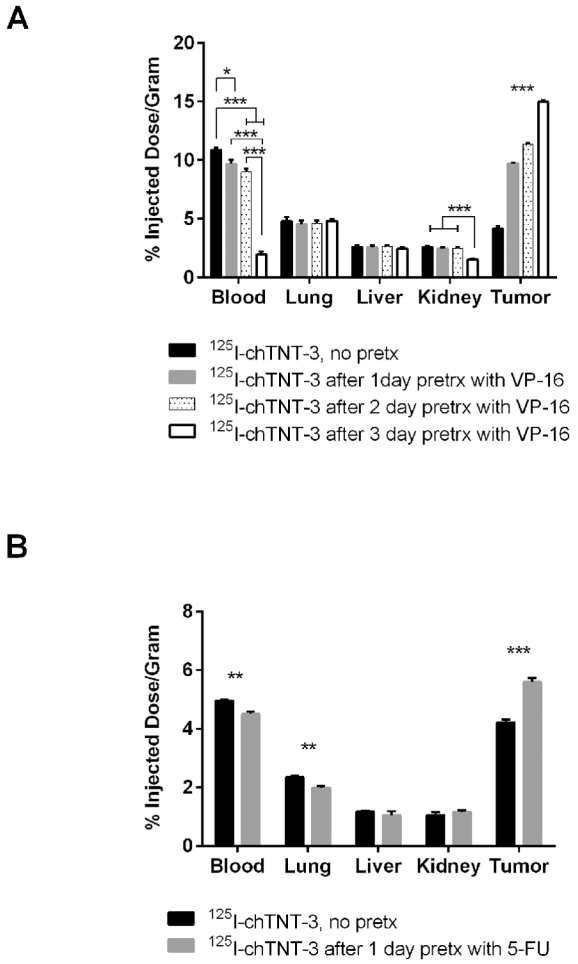

Figure 2.

Three-day biodistribution of ^{125}I-labeled chTNT-3 administered at (**A**) 1 d, 2 d, or 3 d after pretreatment with VP-16 (30 mg/kg) in MAD109 bearing BALB/c mice and (**B**) of ^{125}I-labeled chTNT-3 administered 1 d after 5-FU (50 mg/kg) in LS174T-bearing nude mice. Error bars represent standard error of the mean. * $p < 0.05$, ** $p < 0.01$, *** $p < 0.001$ as determine using one-way ANOVA followed by Tukey's post-hoc test (A) and two-tailed Student's t-test (B). N = 4 mice for all groups.

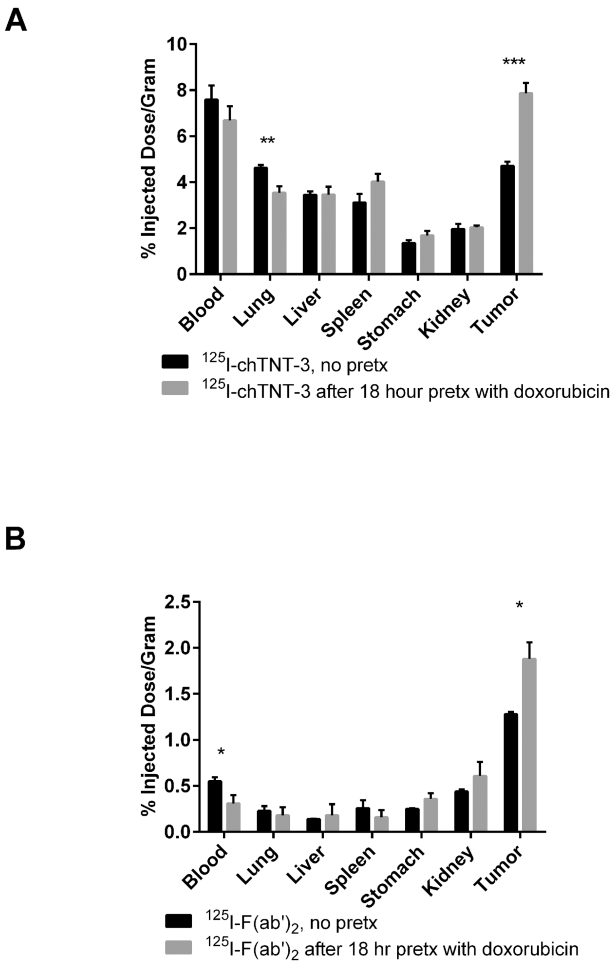

Figure 3.

One-day biodistribution of (**A**) ^{125}I-labeled chTNT-3 with or without a 24 h pretreatment, and (**B**) ^{125}I-labeled F(ab')2 with or without an 18 h pretreatment with doxorubicin (10 mg/kg) in LS174T-bearing nude mice. Error bars represent standard error of the mean. * $p < 0.05$, ** $p < 0.01$, *** $p < 0.001$ as determine using two-tailed Student's t-test. N = 5 mice for all groups.

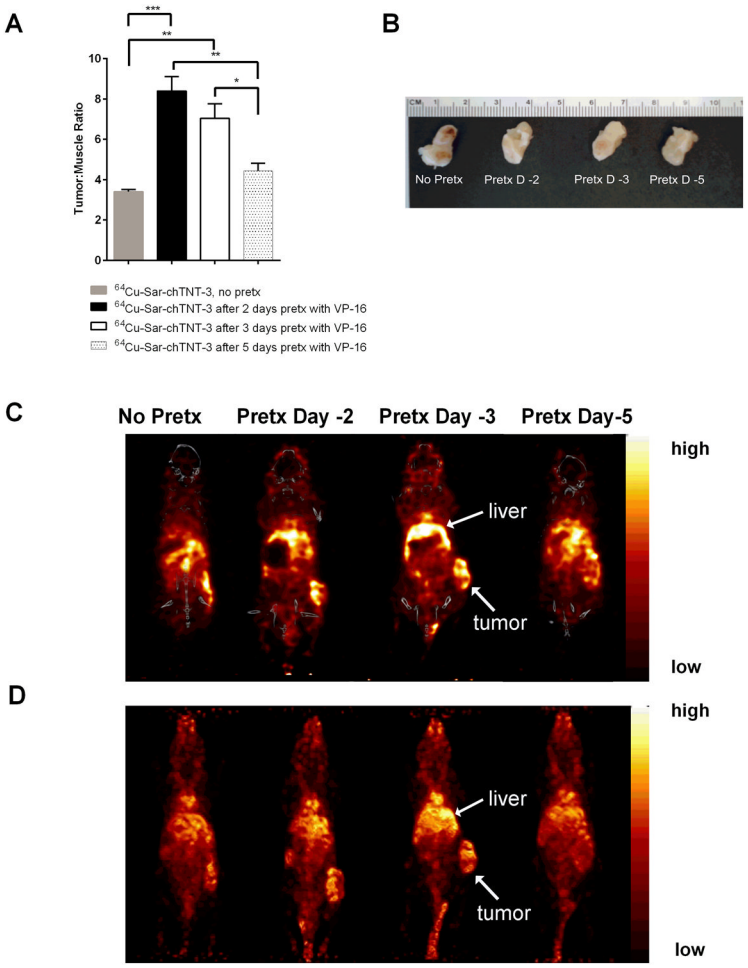

Figure 4.

MicroPET/CT images of ^{64}Cu-Sar-chTNT-3 in MAD109-bearing BALB/c mice following VP-16 pretreatment. (**A**) Tumor to muscle ratios of radioactivity per volume of tissue measured 1 d post-injection of ^{64}Cu-Sar-chTNT-3. Error bars represent standard error of the mean. * $p < 0.05$, ** $p < 0.01$, *** $p < 0.001$ as determine using one-way ANOVA followed by Tukey's post-hoc test. N = 3 mice for all groups. (**B**) Excised tumors from mice shown in **C** and **D**. (**C**) Representative PET/CT coronal sections taken 1 d post-injection of ^{64}Cu-Sar-chTNT-3. (**D**) Representative whole-body PET images taken 1 d post-injection of ^{64}Cu-Sar-chTNT-3. Liver and tumor uptake in **C** and **D** are labeled accordingly.

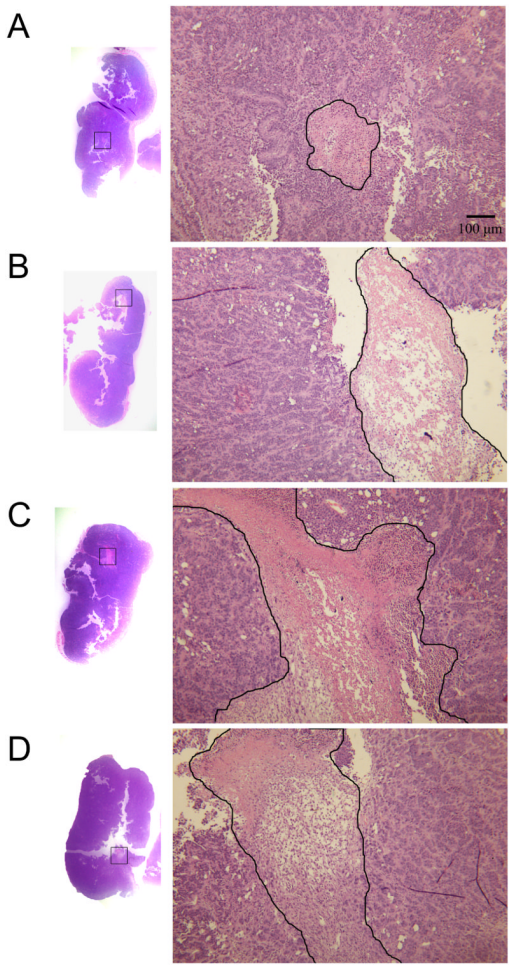

Figure 5.

H&E tissue sections of MAD109 tumors. Representative sections from mice receiving **(A)** no pretreatment, **(B)** VP-16 (30 mg/kg) 2 days prior, **(C)** VP-16 (30 mg/kg) 3 days prior, and **(D)** VP-16 (30 mg/kg) 5 days prior to receiving ^{64}Cu-Sar-chTNT-3. Mice were sacrificed 1 day later and tumors were stained with H&E. The largest areas of necrosis from each section are shown on the right at 40× magnification, with areas of necrosis outlined in black.

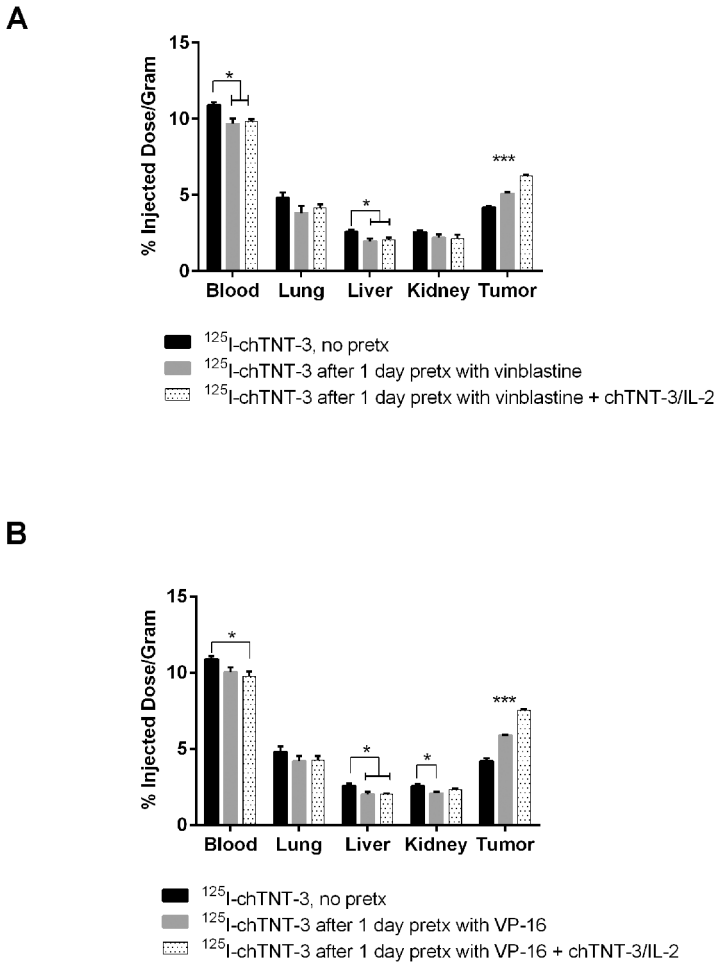

Figure 6.

Three-day biodistribution of I^{125}-labeled chTNT-3 administered 1 d after chemotherapy treatment of MAD109-bearing mice with and without chTNT-3/IL-2 pretreatment. **(A)** Vinblastine (1.4 mg/kg) treatment and **(B)** VP-16 (30 mg/kg) treatment in MAD109 bearing BALB/c mice. Error bars represent standard error of the mean. * $p < 0.05$, ** $p < 0.01$, *** $p < 0.001$ as determine using one-way ANOVA followed by Tukey's post-hoc test. N = 4 mice for all groups.